JOURNAL OF CATALYSIS 69, 180–192 (1981)

Rhodium Cluster Ultradispersed Catalysts of High and Low Activity

W. F. GRAYDON AND M. D. LANGAN

Department of Chemical Engineering and Applied Chemistry, 200 College Street, University of Toronto, Toronto, Ontario M5S 1A4, Canada

Received August 13, 1980; revised December 4, 1980

Catalysts were prepared using $RH_6(CO)_{16}$ adsorbed or slurried on a silica substrate. For these catalysts the rate constants for the reduction of benzene and in some cases cyclohexene were determined. The catalyst particle size distributions were determined by electron microscopy. These results were analyzed to provide varying rate constants assigned to catalyst particles of various sizes. Clusters of rhodium atoms of 0.8 to 1.2 nm corresponding to about Rh_6 were found to have very low, possibly zero, activity for hydrogenation reactions. Clusters of atoms above 1.4 nm diameter were found to be active catalysts for hydrogenation under the same conditions. Some evidence indicating a very high activity for catalyst particles between 1.2 and 2.0 nm was obtained. Below 2.0 nm only two-dimensional rafts are found. This high activity is not therefore attributable to terrace edge sites although evidence of such enhanced activity was found at lower dispersions, 2.0 to 3.0 nm diameter.

INTRODUCTION

Arene hydrogenation is catalyzed by many different metal surfaces. Rhodium metal surfaces as hydrogenation catalyst have been described extensively (*1–8*). The arene reduction reaction is said to be facile (*9*). Only very few indications of homogeneous arene reduction on discrete metal atoms have been reported (*10, 11*). Indeed, even on six-atom clusters, kinetic data for benzene reduction by rhodium have indicated that the cluster may be a very low activity catalyst in both homogeneous and heterogeneous catalytic modes (*12*). Both homogeneous and heterogeneous systems prepared using Rh_6 clusters showed arene reduction activity, but in both modes activity was attributed to aggregation of clusters or even metallic particulates arising from Rh_6 clusters. $Rh_6(CO)_{16}$ supported on a polymer matrix was reported to be inactive as a catalyst in the reduction of benzene (*7, 13*). The activity observed was interpreted as probably the result of metal agglomeration.

The study of the chemistry of the Rh_6 clusters on various supports (*12, 14–16*) was undertaken in the expectation that the cluster compounds would provide well-dispersed models of heterogeneous metal catalysts and also serve to provide a link between heterogeneous and homogeneous catalytic systems.

A long-time goal in catalysis has been to disperse a metal onto a surface in such a way that every metal atom is a surface atom and hence accessible to the reaction (*17–20*). A measure of success in achieving this state of dispersion is the ratio of metal surface atoms to total metal atoms. It has been shown that in many systems attempts to attain 100% dispersion, or "atomic dispersion," cause the metal particles to break down into small, two-dimensional clusters which have been designated rafts (*17*). Electron microscope studies coupled with chemisorption and infrared spectroscopy have revealed that in the case of supported rhodium, rafts can be as large as 4.0 nm in diameter and can contain more than 80 atoms (*17*). These studies also revealed that all rhodium particles are rafts for diameters smaller than 2.0 nm. Similar results have been reported for other metals (*20*). If one assumes an interatomic spacing of 0.375 nm for rhodium (*17, 18*), then a 2.0-nm circular raft contains 14 atoms. From this work one

0021-9517/81/050180-13$02.00/0

can infer that atomic dispersion is obtained once one obtains rafts containing fewer than 14 atoms.

Once atomic dispersion has been attained, making smaller rafts will not enhance dispersion, but it may alter the metallic properties of the system of the metal atom rafts. Single metal atoms are not metals. Using molecular orbital calculations, Baetzold (*21, 22*) concluded that silver clusters containing as many as 55 atoms have metal-like properties but are not metals and that, at 20 atoms, the bond energy is only one-third the cohesive energy of the bulk metal. Coupled with the loss of metallic property is the increased proportion of edge atoms. Seven-atom rafts are entirely made up of edge atoms and sixteen-atom rafts are still 75% edge atoms (*17*). Chemisorption studies indicate that rhodium edge atoms enjoy greater steric freedom than the other atoms enabling them to absorb two CO molecules when the others are limited to one CO molecule.

In this paper we will examine various Rh_6-supported cluster catalysts for benzene reduction in order to determine the relationship between aggregation and catalytic activity.

EXPERIMENTAL METHODS

Materials

Rhodium carbonyl ($Rh_6(CO)_{16}$) was obtained from Johnson Matthey and was kept under an argon atmosphere. A nonporous Aerosil silica (200 m^2 g) dried under vacuum at 350°C for 12 hr was used as the support. Argon and ultrahigh-purity hydrogen (99.999% H_2 purity <0.2 ppm O_2 <0.2 ppm N_2, no other impurities) were supplied by Matheson. "Baker Instra-Analyzed" benzene was used as a solvent in catalyst preparation and as a reagent in the kinetic studies.

Preparation of Catalysts

Two types of catalysts were prepared: slurry catalysts and precipitation or dissolved metal catalysts.

The slurry catalysts were prepared by slurry-depositing $Rh_6(CO)_{16}$ onto the silica support at 353°K in benzene under an argon atmosphere. The benzene solvent was removed by filtration and evaporation under vacuum.

The ultradispersed catalysts were prepared in a Soxhlet extractor tube. The silica was suspended in 50 cm^3 of benzene and placed in the extraction flask. The solution was heated to 353°K and the benzene was refluxed through finely ground rhodium carbonyl in a Whatman extractor thimble. The mass of $Rh_6(CO)_{16}$ placed in the extraction thimble was varied from 7 to 30 mg. The total benzene reflux time was varied from 1 to 80 hr in order to vary the final concentration and the particle size of the rhodium on the silica.

For all catalysts, rhodium concentrations were measured by neutron activation analysis. The analysis was done on four samples from each catalyst. All concentrations were accurate to within a SD of ±6%. Concentrations were confirmed by simple mass balance considerations for all slurry catalysts. Particle sizes were measured on transmission electron micrographs.

The Kinetic Apparatus

A flowchart of our equipment is given in Fig. 1. Hydrogen and argon flow rates were controlled by Brooks model 8944 pneumatic flow controllers (I,II,III). Hydrogen was passed in series through flow controller (II), a benzene saturator (1), a condenser (2), a fluidized bed differential reactor (3), the gas–liquid chromatography sampling valve (4), and a soap-film flowmeter (6).

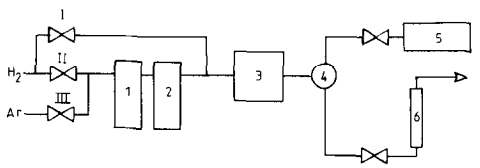

FIG. 1. Apparatus for determining the kinetics of benzene hydrogenation. (1) Saturator, (2) condenser, (3) reactor, (4) gas sampling valve, (5) gas–liquid chromatograph, (6) soap-film flowmeter.

The saturator operated at room temperature. The condenser was thermostated at 10°C which corresponds to a benzene partial pressure of 45.6 Torr. Benzene partial pressures were varied by diluting the reactant stream with hydrogen downstream of the condenser via flow controller (I). Hydrogen partial pressures were varied by diluting the hydrogen stream with argon via flow controller (III). The reactor was a 5-mm-i.d. Pyrex-glass U-tube immersed in a thermostated constant-temperature water bath (±0.5°C). The catalyst samples rested on a porous glass disk and weighed from 9 to 12 mg.

Products were analyzed by flame ion detection using a Varian Aerograph 1860-1 gas chromatograph equipped with an 8 ft × 0.125 in.-OD column packed with 15% polyethylene glycol 600 on Chromosorb. The column was maintained at 25°C (298°K).

Flow rates were measured with the soap film flowmeter (*6*). Product stream flow rates varied from 0.30 to 0.37 ml/s. Hydrogen pressures were varied from 80 to 700 Torr (1 Torr = 133.3 Nm^{-2}); benzene pressures from 10 to 45.6 Torr. Catalytic activities are expressed in gram moles of cyclohexane per second per gram of rhodium. Conversions were kept below 5% except at low benzene pressures (~10 Torr) when conversions reached 10%.

Electron Microscope

All electron micrographs were made using a Philips 300 transmission electron microscope equipped with high-resolution pole pieces. Kodak electron image plates were used.

Pictures were usually taken at a magnification of 205,200× using 80-kV electrons although higher magnifications were occasionally used with 100-kV electrons. The microscope was calibrated using the 002 spacing (0.344 nm) of graphitized carbon black. Contrast was maximized by placing a 30-μm aperture in the objective lens (*18*). The coherency of the electron beam was maximized by using a pointed filament. Contamination was minimized by using liquid nitrogen to cool the specimen stage.

Samples to be examined were ultradispersed in ethanol for 10 min (3 mg/5 ml), deposited onto holey Formvar films supported on 400 or 1000 mesh grids, and dried at room temperature. Carbon coating was not necessary.

All micrographs were taken over holes to eliminate background noise.

RESULTS

Kinetics of Benzene Reduction

The reduction of benzene using heterogeneous catalysts is known to be very complex. The complex nature of the kinetics has been verified over a wide range of experimental conditions by Van Meerten and Coenen (*23*). Mechanisms for this process have been proposed based on restricted ranges of conditions but no mechanism of general validity has been given, even for nickel catalysts for which a great deal of kinetic data is available.

Our benzene reduction studies using rhodium catalysts show a similar complexity to that which has been reported for nickel. For example, a maximum in the rate-versus-temperature plot was noted at high temperatures for some types of rhodium catalyst. The kinetic data reported here are presented as the empirical basis for the comparison of various rhodium catalyst preparations. Determinations of "catalyst activity" without a knowledge of the empirical kinetic equations were found to be very difficult to correlate.

The effect of benzene and hydrogen pressures on the rates of reduction of benzene over two typical catalysts are given in Figs. 2 and 3.

The dependence of benzene hydrogenation activity on hydrogen pressure is shown in Fig. 2 for 0.30% Rh/SiO_2 and 0.88% Rh/SiO_2 catalysts. The benzene partial pressure was fixed at 45.6 Torr and the

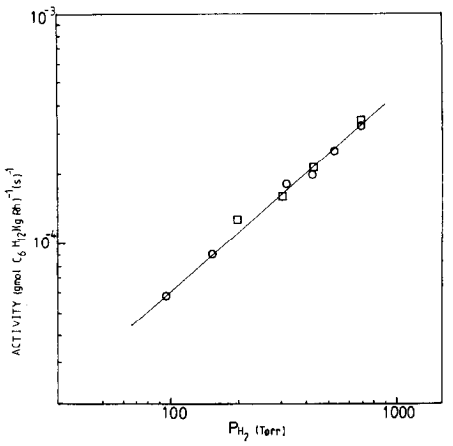

FIG. 2. Dependence of benzene hydrogenation activity on hydrogen partial pressure. Catalysts: (□) 0.30% Rh/SiO_2, (○) 0.88% Rh/SiO_2. Reaction temperature: 35°C. Benzene partial pressure: 45.6 Torr.

reaction temperature at 308°K. Hydrogen partial pressure was varied from 98 to 715 Torr by diluting the hydrogen with argon. Measurements were taken at room temperature.

The dependence of benzene hydrogenation activity on benzene partial pressure for the same two catalysts is shown in Fig. 3. The benzene partial pressure was varied from 10 to 45.6 Torr. However, no diluting gas was used so the hydrogen pressure was allowed to vary over the range 715–750 Torr such that the total pressure of the benzene–hydrogen mixture was atmospheric pressure. The reaction temperature was 308°K.

These kinetic data may be summarized as reaction orders of 0.85 with respect to hydrogen and 0.42 with respect to benzene.

We know of no previous study of reaction orders for benzene hydrogenation over supported rhodium. Some benzene reduction reaction orders have been reported for other supported metals. Badilla-Ohlbaum *et al.* (*24*) report an order in hydrogen greater than 2 at 130°C for Fe/Al_2O_3 catalysts. Taylor and Staffin (*25*) report hydrogen orders of 1.0–1.6 and benzene orders of 0.1–0.3 for a 5% Ni/SiO_2 catalyst over a temperature range of 353–399°K. Van Meerten and Coenen (*23*) report that for a 11.3% Ni/SiO_2 catalyst the hydrogen orders range from 0.5 to 0.7 at temperatures below 373°K to orders as high as 3 at 473°K. Benzene orders varied from 0.1 to 0.5 over the same range. Van Meerten also quotes a number of papers reporting hydrogen orders from 0.5 to 3 and benzene orders from 0.1 to 0.5 at temperatures ranging from below 100°C to 250°C. The values reported in this work fall within the range reported by Van Meerten although the benzene order falls near the upper end of the scale, a region usually reserved for the higher-temperature kinetics.

These kinetic data are similar to published data for benzene reduction over other heterogeneous catalysts. It seems likely that the mechanisms involved in the rhodium catalysis are not substantially different from those governing other heterogeneous benzene reductions. We suppose therefore that the effects of variation in rhodium catalyst aggregation parameters may be widely applicable.

In order to support this expectation further the effect of temperature variation on the reaction rate was determined as shown in Fig. 4. Some literature data are available for the temperature dependence of benzene reduction over rhodium catalysts on different supports. An activation energy of 9.2 kcal/mol was reported by Völter *et al.* (*1*) for a 0.54% Rh/MgO catalyst. Sokol'skii *et al.* (*5*) measured activation energies ranging from 5.7 to 7.2 kcal/mol for Rh/Al_2O_3

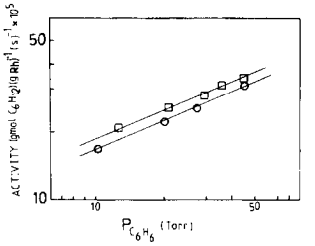

FIG. 3. Dependence of benzene hydrogenation activity on benzene partial pressure. Catalysts: (□) 0.30% Rh/SiO_2, (○) 0.88% Rh/SiO_2. Reaction temperature: 35°C. Hydrogen partial pressure: 715–750 Torr.

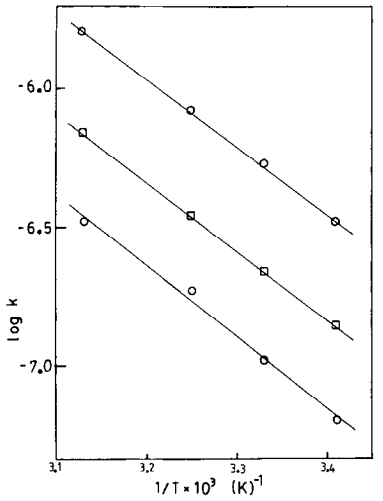

FIG. 4. Arrhenius plots showing the dependence of benzene hydrogenation activity on temperature. Catalysts: (O) 0.45% Rh/SiO_2, (○) 0.88% Rh/SiO_2, (□) 2.68% Rh/SiO_2. Hydrogen partial pressure: 715 Torr. Benzene partial pressure: 45.6 Torr.

catalysts ranging from 0.25 to 5% rhodium. Studies examining benzene kinetics over other supported metals report.benzene hydrogenation activation energies varying from 4.5 to 13 kcal/mol (*9, 23–28*). The data reported in Fig. 2 give activation energies of benzene hydrogenation for three Rh/SiO_2 catalysts. The activation energies vary from 5.4 to 6.3 kcal/mol which is in good agreement with the range reported by Sokol'skii.

In summary, our kinetic data may be expressed as

$$r = kP_B^{0.42}P_H^{0.85}, \qquad k = ae^{-5900/RT}. \quad (1)$$

This empirical rate expression is well within the ranges which have been published for the heterogeneous catalysis of benzene reduction over a wide variety of supported metal catalysts.

For many of the highly dispersed catalysts only monolayer rafts are observed. For these catalysts a turnover number based on the assumed accessibility of all rhodium atoms can be calculated. These are given in Table 1 with literature values for other metal catalysts as comparison.

Electron Microscopy

Typical electron micrographs at a magnification of 615,600× are given in Figs. 5 and 6. These micrographs show two qualitatively different types of catalyst aggregation on the silica substrate. At highest dispersions, only apparently two-dimensional rafts can be observed. The two dimensionality is inferred from the constant optical density over the substrate of the rhodium particles. At slightly lower dispersions, a mixture of dark and light particles can be seen on substrate regions of constant optical density indicating that both two-dimensional and three-dimensional particles are

TABLE 1

Turnover Numbers and Activities for Benzene Hydrogenation for Various Catalysts

Catalyst	Temperature (°C)	Turnover number (hr^{-1})	Dispersion (%)	Activity (g mol C_6H_6) (g mol metal)$^{-1}$(hr)$^{-1}$	Reference
Rh/SiO_2	35	37–160	100	37–160	This work
Rh/polymer	rt	4.2	—	—	(*2*)
$[Rh(\eta^5\text{-}C_5Me_5)Cl_2]_2$	50	11.1	—	—	(*3*)
Rh/MgO	40–70	—	—	141	(*1*)
Pt/Al_2O_3	85	760–780	8–85	62–663	(*26*)
Pt/Al_2O_3	50	800	12–67	96–536	(*9*)
Pt/SiO_2	127	301	18	54	(*27*)
Ru/SiO_2	127	720	26	187	(*27*)
Re/SiO_2	127	2	20	0.4	(*27*)
Fe/Al_2O_3	130	—	—	2	(*24*)
Ni/SiO_2	25	3.0–4.7	13–60	0.4–2.6	(*31*)

FIG. 5. Transmission electron micrograph of a very highly dispersed Rh/SiO_2 catalyst (catalyst 2 in Fig. 8 and 10). All rhodium appears in the form of two-dimensional rafts (——). Original magnification: 615,600×.

present. Similar observations have been reported (*17*) for other rhodium catalysts. Within some of the darker particles, two density levels can be distinguished suggesting the presence of three-dimensional, terraced structures. These three-dimensional, terraced catalyst particles were never observed in catalyst preparations having an average raft diameter below 1.8 nm and were only rarely observed for average diameters up to 2.4 nm. These observations for the cluster rhodium carbonyl catalysts on a silica substrate are very similar to those observed by Yates *et al.* (*17*) for rhodium catalysts prepared from mononuclear $RhCl_3$ on an alumina substrate, indicating that the deposition of the rhodium atoms in six-atom clusters does not markedly affect the types of catalyst particles formed. Indeed, the transition diameter at which three-dimensional terraced structures first appear is almost the same for these catalysts and for those previously reported (*17*).

For all catalysts examined, both the degree of dispersion and the types of particles observed did not appear to depend on the catalyst loading (see Table 2). At low average raft diameters, below 1.8 nm, only two-dimensional rafts were observed without apparent effect of catalyst loading from 0.64 to 1.49% Rh by weight. The same lack of dependence on catalyst loading was observed for the terraced, three-dimensional particles which appeared only when the average raft diameter exceeded 1.8 nm at loadings varying from 0.44 to 2.63% Rh by weight.

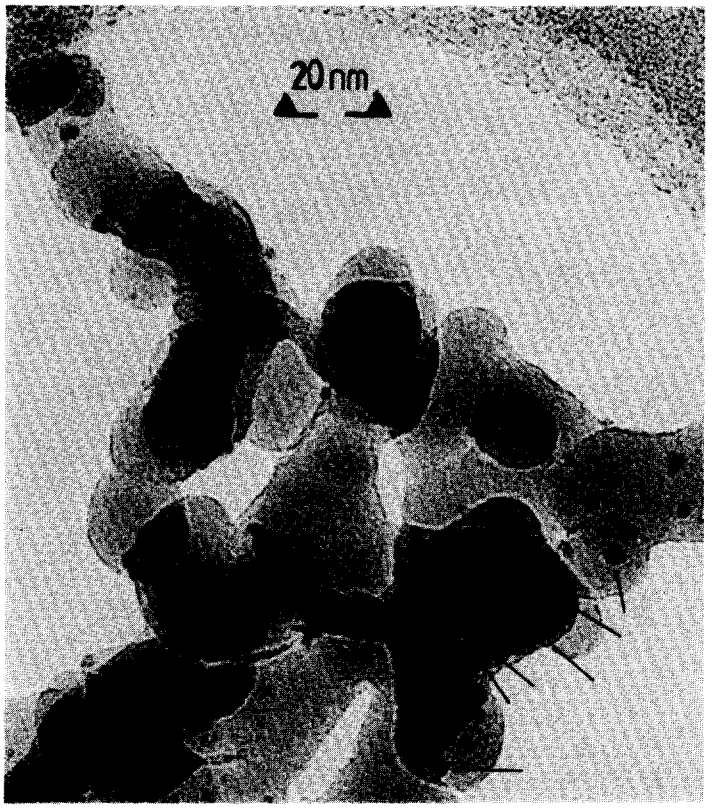

FIG. 6. Transmission electron micrograph of a dispersed Rh/SiO_2 catalyst for which both apparently two-dimensional and three-dimensional rhodium particles (——) are visible (catalyst 11 in Figs. 8 and 10). Original magnification: 615,600×.

For comparison, some rhodium cluster catalysts of large average Rh particle diameter (30–120 nm) were prepared in the same loading range. As may be seen from Fig. 7, the catalyst particles, although large, are quite porous, being made up of aggregates of microparticles roughly 2.0 nm in diameter. This physical form may result from the large mass of carbon monoxide removed from the cluster carbonyl during catalyst preparation. Such catalysts showed increasing rates with time which were supposed to result from decarbonylation. Catalysts prepared by adsorption all showed rates which were constant for several hours with no initial increase in rates.

TABLE 2

The Average Diameters and Loadings of the Rhodium Catalysts for Fig. 10

Catalyst	Loading (% Rh by wt.)	Average diameter (nm)
1	1.49	1.10
2	0.86	1.35
3	0.96	1.51
4	0.64	1.63
5	2.63	2.02
6	0.44	2.20
7	1.25	2.46
8	0.93	2.54
9	2.20	2.54
10	0.45	2.54
11	0.74	2.63

Particle sizes for six rhodium atoms may be expected to lie between 0.8 nm if the bipyramidal form is retained in the Rh_6 crystallite (Fig. 9a) and 1.38 nm for close-packed monolayer rafts of six atoms. At the highest dispersion, the distribution indicates that the catalyst consisted largely of

FIG. 7. Transmission electron micrograph of a Rh/SiO_2 slurry catalyst. Original magnification: 615,600×.

0.8- to 1.2-nm-diameter particles which we assume to be clusters of six rhodium atoms. Several catalysts have a large fraction of six-atom particles. All these catalysts show average diameters below 1.8 nm. For catalysts having particles of larger diameter, the fraction of 0.8- to 1.2-nm particles becomes very small. Of course particles smaller than 0.8 nm may be present but unobserved and some evidence of even mononuclear fragments from Rh_6CO_{16} has been reported (*29*).

The diameters to be associated with two-, three-, and four-cluster aggregates are matters for greater conjecture, even assuming that the clusters do not break up but provide aggregates in multiples of six rhodium atoms. At least, it seems reasonable to assume that three or more clusters will produce particles having diameters of 2.0 nm or greater. Many of these larger catalyst particles have been observed to have essentially a two-dimensional raft structure, even up to diameters of 3.5 nm. Particle size distributions are shown in Fig. 8.

Catalyst Activity and Particle Area

In Fig. 10 are plotted the rate constants from Eq. (1) versus the average catalyst particle cross-sectional areas as determined from the distribution plots. The activity values are each averages of at least 30 individual rate-constant measurements and each of the distribution plots involved the measurement of more than 200 individual rhodium particle diameters on four micrograph plates. Replicate size distribution determinations have indicated an average deviation from the mean for individual rod heights of ±10% from plate to plate. We

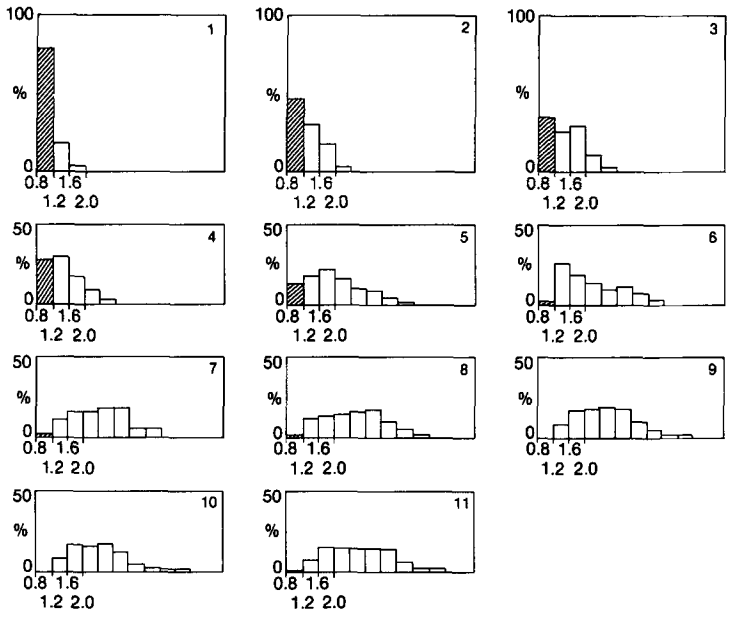

FIG. 8. Particle size distributions for the Rh/SiO_2 catalysts listed in Table 2 determined by electron microscopy.

thus estimate the reliability of the rod heights in these size distributions which are the average of three or four plates to be about ±5%. Similar or better precision is expected for the rate data. For that portion of Fig. 10 in which the catalyst particles are characterized by two-dimensional raft structures, the data show a reasonably consistent correlation. Each point on this graph represents the activity and average particle diameter of an independently prepared catalyst. The average diameter for each catalyst is calculated from a unique and changing distribution of particle sizes characteristic of that catalyst. Because of variations in size distribution, it is not surprising that the activity is not a smooth function of average particle diameter.

DISCUSSION

An examination of Fig. 10 shows a fairly monotonous decrease in observed rate constant with decreasing average particle diameter even for that region below 2 nm diameter in which the literature and our own observations indicate only two-dimensional raft structures. The scatter is rather larger than we would have expected and no account has been taken of the marked skewing of the distribution as average particle diameter decreases. Since the dependence of rate constants on size of particle seems significant perhaps the data may be subject to more detailed analysis by permitting various particle sizes within one catalyst to be characterized by various rate constants. The size distributions would then permit a simple sum of rates for the "mixed catalyst" to give the overall rate recorded on Fig. 10. This speculation has been tried by allowing each catalyst to be considered as a mixture of two, three, or four catalysts with undetermined rate constants and solving for the rate constants by using sets of two, three, or four measured total rates for the assumed "mixed catalyst" as shown by the distributions. The results are given in Table 3. A remarkable result of these calculations is the uniformly small rate constant associated with particles of 0.8 to 1.4 nm diameter. A second, and only slightly less striking conclusion, is that all particle sizes larger than 1.2 nm diameter have large rate

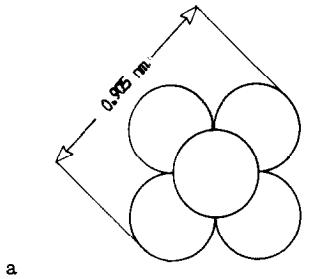

a

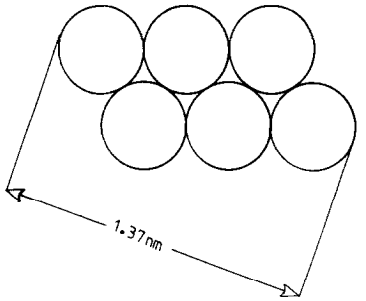

b

FIG. 9 (a) Projection of a bipyramidal arrangement of six rhodium atoms. (b) A close-packed monolayer raft of six atoms. Maximum dimensions for (a) and (b) are based on a measured average packing spacing of Rh on SiO_2 of 0.375 nm (*17, 18*).

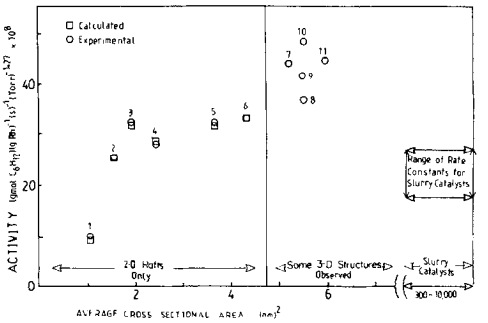

FIG. 10. Measured and calculated rate constants as a function of the average catalyst particle cross-sectional area.

constants calculated. A third and more doubtful observation is the very large values of rate constant calculated for 1.2- to 2.0-nm diameter particles. As the data in Table 3 have indicated, the original data of Fig. 10 could be fitted by the assumption that each catalyst in a mixture of three catalysts has the rate constants as shown 0.8–1.4 nm, $k_1 = 0$; 1.4–2.0 nm, $k_2 = 75$; and >2.0 nm, $k_3 = 16$ in the units and magnitudes of Fig. 10. The calculated results are plotted in Fig. 10 and indicate that the scatter may not be wholly random but rather determined by differences in the distribution at different-sized particles. The best two-constant fit used $k = 0$ for "single-cluster" particles (0.8–1.2 nm) and $k = 40 \times 10^{-8}$ (g mol C_6H_6)(g Rh)$^{-1}$(s)$^{-1}$(Torr)$^{-1.27}$ for particles greater than 1.2 nm. This fit is tabulated in Table 4. It is much less satisfactory than the three-constant fit. However, even this fit may be within the precision of the measured values. For this reason we view the high rate constant assumed for two-cluster particles (1.2 to 2.0 nm) in the three-constant fit as indicated only. The assignment of $k = 0$ to the 0.8- to 1.2-nm particles seems well founded.

TABLE 3

Calculation of Rate Constants for Particle Sizes from the Distribution Chart

Two-rate-constant equations					Three-rate-constant equations				Four-rate-constant equations			
Particle diameter (nm)	(1)	(2)	(3)	(4)	Particle diameter (nm)	(5)	(6)	(7)	Particle diameter (nm)	(8)	(9)	(10)
k_1 (0.8–1.2)	−0.8	−1.9	−0.6	1.1	k_1 (0.8–1.2)	−10.1	−1.9	−4.3	k_1 (0.8–1.2)	0.1	0.1	−0.8
k_2 (>1.2)	49.1	31.5	48.3	47.5	k_2 (1.2–1.6)	99.9	58.1	70.1	k_2 (1.2–1.6)	52.1	45.5	50.6
					k_3 (>1.6)	2.2	39.7	29.0	k_3 (1.6–2.0)	68.9	65.1	56.1
									k_4 (>2.0)	9.2	15.8	22.2

Note. k_t (g mol)(g Rh)$^{-1}$(s)$^{-1}$(Torr)$^{-1.27} \times 10^8$. (1) Catalysts 1 and 2; (2) catalysts 1 and 3; (3) catalysts 1 and 4; (4) catalysts 2 and 4; (5) catalysts 1, 2, and 3; (6) catalysts 1, 2, and 4; (7) catalysts 1, 2, and 7; (8) catalysts 1, 2, 3, and 4; (9) catalysts 1, 2, 4, and 5; (10) catalysts 1, 2, 4, and 6.

TABLE 4

A Two-Constant Fit to the Activities of the Two-Dimensional Raft Catalysts of Fig. 10

Catalyst	Measured rate constant ((g mole C_6H_6)(g Rh)$^{-1}$(s)$^{-1}$(Torr)$^{-1.27}$ × 10^8)	Calculated rate constant ((g mole C_6H_6)(g Rh)$^{-1}$(s)$^{-1}$(Torr)$^{-1.27}$ × 10^8)
1	10	9
2	26	21
3	32	26
4	28	28
5	32	34
6	33	39

Note. Single-cluster particles (0.8–1.2 nm): k assuamed = 0 (g mol C_6H_6)(g Rh)$^{-1}$(s)$^{-1}$(Torr)$^{1.27}$. Larger particles (>1.2 nm): k assumed = 40 × 10^{-8} (g mol C_6H_6)(g Rh)$^{-1}$(s)$^{-1}$(Torr)$^{1.27}$.

For that portion of Fig. 10 above 2.4 nm average diameter, all samples showed some three-dimensional terraced structures and rate constants (activities) were larger and more variable. These observations are in very good agreement with the behavior reported by Yates *et al.* (*17*) for mononuclear rhodium on alumina. These authors state that both rafts and three-dimensional particles were observed in the range 2.0–4.0 nm. The three-dimensional particles observed for clusters frequently exhibit an apparent terraced structure with sharp increases in optical density observable within the area of a large raft. If present, such terrace structures would be expected to show an enhanced adsorption and an increased catalytic rate (*30*). Calculation for the number of terrace edge (B5) sites on octahedral nickel crystals (*31*) shows that the number of such sites increases with decreasing crystallite size to a maximum at about 2.0 nm equivalent spherical diameter and drops sharply to zero below that value. The drop in the activity of the rhodium cluster catalysts observed on transition from terraced to two-dimensional structures at about 2.0 nm is qualitatively similar. The scatter of the three-dimensional data may therefore result from the activity associated with an unknown fraction of active terrace edge sites. Below about 2 nm diameter, rhodium cluster particles are two dimensional and there are no terrace edge sites. However, there are still edge atoms of rhodium over silica which may show an enhanced adsorption relative to the central atoms (*17*). Our analysis of our data leads us to accept that particles below 1.4 nm diameter are catalytically inactive, while those above 1.4 nm diameter are fully active. Indeed particles between 1.4 and 2.0 nm diameter may show very large activity though this is more speculative than the first two observations. Similar data have been reported for benzene reduction on nickel (*32*). These are shown for comparison in Fig. 11. These authors (*32*) regard the increase in activity as diameters drop from 5.0 to 1.2 nm as established but express some doubt about the reality of the fall in activity for smaller particles. Our data confirm the low activity of small rhodium catalyst particles below about 1.2 nm for arene reduction. As may be seen in Fig. 11, rhodium particles are not effective catalysts below diameters of 1.2–1.4 nm. For

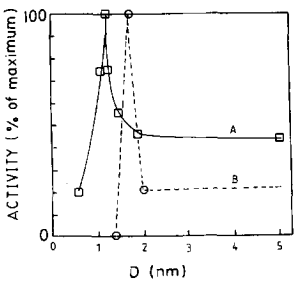

FIG. 11. Relation between catalytic activity and crystallite size for Ni/SiO_2 catalysts A (*32*) and for Rh/SiO_2 catalysts B.

mononuclear nickel crystallites, the activity reported is high down to 1.0 nm. Crystallite sizes in the nickel catalyst work were assumed proportional to loading and therefore crystallite sizes were subject to questions about the influence of loading (*32*). In the rhodium work, crystallite sizes were not related to loading in any noticeable fashion.

These observations add to a growing body of evidence that not only are single metal atoms generally ineffective for arene reduction (*10, 11*) but also small aggregates of atoms are similarly ineffective. $Rh_6(CO)_{13}(P Ph)_3$ and $Rh_6(CO)_{10}(P Ph)_6$ are inactive in homogeneous solution as is the relatively insoluble $Rh_6(CO)_{16}$ (*12*). However, similar catalysts, $Rh_6(CO)_{16}$ on phosphinated silica, were active for arene reduction (*12*). The presence of metallic rhodium was postulated as the source of this activity for the heterogeneous catalyst, but no discussion of rhodium dispersion and the metallic property was given.

The exchange of $Rh_6(CO)_{16}$ on phosphinated polymers (*7, 13*) produced catalysts which showed some activity for arene reduction. The authors state that this activity is "probably an indication that agglomeration of the metal had occurred to a small extent" (*13*).

Thus, all arene reduction activity of rhodium catalysts except for the mononuclear homogeneous case has been imputed to metallic crystallites of unspecified nuclearity. Our data show that ultradispersed, two-dimensional aggregates with as few as 12 rhodium atoms (two clusters) are catalytically active for arene reduction. There is even some indication that 12-atom rhodium raft crystallites are more active than larger rafts containing 18 or more atoms. These observations are for raft crystallites which seem to be two dimensional. Therefore the enhanced activity probably cannot be attributed to terrace edge sites.

Jarrell and Gates (*13*) noted that "it is tempting to consider the occurrence of arene hydrogenation as a demonstration of the presence of catalytic species having metal-metal bonds." If we yield to this temptation, we would suppose that the transition to sufficient metal bonding for the zero-valent adsorbed rhodium in two-dimensional rafts occurs between 6 and 12 atoms.

This sharp reduction in catalytic effectivity between 6 and 12 rhodium atoms per raft is not limited to arene reduction. Low activities have been reported for ethane hydrogenolysis over rhodium catalysts in an extremely high state of dispersion (1.1 nm) by Yates and Sinfelt (*19*) who also note that high catalytic activity appears to be associated with an intermediate state of dispersion of the metal. As may be seen in Table 5, a similar but not quite so sharp reduction in catalytic activity for cyclohexene was also observed. The ratios of activities for cyclohexene to benzene reduction fall within the range of reported values (*7, 12*) and show no marked trend.

The conclusion is strengthened that 12

TABLE 5

Activities of Rh/SiO_2 Catalysts for Hydrogenation of Benzene and Cyclohexene at 35°C

Catalyst[a]	Benzene hydrogenation rate ((g mol C_6H_6)(g Rh)$^{-1}$(s)$^{-1}$ × 10^5)	Cyclohexene hydrogenation rate ((g mol C_6H_6)(g Rh)$^{-1}$(s)$^{-1}$ × 10^5)	Rate of cyclohexane hydrogenation/rate of benzene hydrogenation
1	13.5	2100	156
6	44	3400	77
11	54	6000	111

[a] See Fig. 9.

atoms of zero-valent rhodium in a catalyst particle are sufficient to catalyze hydrogenation reactions, while 6-atom clusters probably are not catalysts.

REFERENCES

1. Völter, J., Hermann, M., and Heise, K., *J. Catal.* **12,** 307 (1968).
2. Holy, N. L., *J. Org. Chem.* **44,** 239 (1979).
3. Russell, M. J., White, C., and Maitlis, P. M., *Chem. Commun.* 428 (1977).
4. Baltzly, R., *J. Org. Chem.* **41,** 920 (1976).
5. Sokol'skii, D. V., Popov, N. I., and Andreichenko, G. I., *Neftekhimiya* **15,** No. 4, 499 (1975).
6. Polkovnikov, B. D., and Khidenel, M. L., *Dokl. Akad. Nauk SSSR* **181,** 25 (1968).
7. Jarrell, M. S., Gates, B. C., and Nicholson, E. D., *J. Amer. Chem. Soc.* **100,** 5727 (1978).
8. Guyot, A., Graillat, Ch., and Bartholin, M., *J. Mol. Catal.* **3,** 39 (1977).
9. Basset, J. M., Dalmai-Imelik, G., Primet, M., and Mutin, R., *J. Catal.* **37,** 22 (1975).
10. Muetterties, E. L., and Hirsekorn, F. J., *J. Amer. Chem. Soc.* **96,** 4063 (1974).
11. Hirsekorn, F. J., Rakowski, M. C., and Muetterties, E. L., *J. Amer. Chem. Soc.* **97,** 237 (1974).
12. Smith, A. K., *et al., in* "Fundamental Research in Homogeneous Catalysis" (Tsutsui, Ed.), Vol. 3, p. 621. Plenum, New York, 1979.
13. Jarrell, M. S., and Gates, B. C., *J. Catal.* **54,** 81 (1978).
14. Smith, A. K., *et al., Inorg. Chem.* **18,** 3104 (1979).
15. Bilhou, J. L., *et al., J. Mol. Catal.* **8,** 411 (1980).
16. Bilhou, J. L., *et al., J. Organometal. Chem.* **153,** 73 (1979).
17. Yates, D. J. C., Murrell, L. L., and Prestridge, E. B., *J. Catal.* **57,** 41 (1979).
18. Prestridge, E. B., and Yates, D. J. C., *Nature* **234,** 345 (1971).
19. Yates, D. J. C., and Sinfelt, J. H., *J. Catal.* **8,** 348 (1967).
20. Prestridge, E. B., Via, G. H., and Sinfelt, J. H., *J. Catal.* **50,** 115 (1977).
21. Baetzold, R. C., *J. Chem. Phys.* **55,** 4363 (1971).
22. Baetzold, R. C., *in* "Advances in Catalysis and Related Subjects," Vol. 25, p. 1. Academic Press, New York/London, 1974.
23. Van Meerten, R. Z. C., and Coenen, J. W. E., *J. Catal.* **37,** 37 (1975).
24. Badilla-Ohlbaum, R., Neuburg, H. J., Graydon, W. F., and Phillips, M. J., *J. Catal.* **47,** 273 (1977).
25. Taylor, W. F., and Staffin, H. K., *Trans. Faraday Soc.* **63,** 2309 (1967).
26. Van Meerten, R. Z. C., Morales, A., Barbier, J., and Maurel, R., *J. Catal.* **58,** 43 (1979).
27. Kubicka, H., *J. Catal.* **12,** 223 (1968).
28. Moss, R. L., Pope, D., Davis, B. J., and Edwards, D. H., *J. Catal.* **58,** 206 (1979).
29. Thornton, E. W., Knozinger, H., Tesche, B., Rafalko, J. J., and Gates, B. C., *J. Catal.* **62,** 117 (1980).
30. Somorjai, G. A., *Catal. Rev.* **7,** 87 (1973).
31. Van Hardeveld, R., and Van Montfoort, A., *Surface Sci.* **4,** 396 (1966).
32. Coenen, J. W. E., Van Meerten, R. Z. C., and Rijnten, H. Th., *in* "Proceedings, 5th International Congress on Catalysis, Florida, 1972" (J. W. Hightower, Ed.), p. 671. North-Holland/Amer. Elsevier, Amsterdam/New York, 1973.